International Journal of Bioprinting

RESEARCH ARTICLE

Fabrication of lumen-forming colorectal cancer organoids using a newly designed laminin-derived bioink

Rosario Pérez-Pedroza[1,2†], Fatimah Al-Jalih[1,2†], Jiayi Xu[1,2], Manola Moretti[1,2], Giuseppina R. Briola[1], Charlotte A. E. Hauser[1,2*]

[1]Laboratory for Nanomedicine, BESE, King Abdullah University of Science and Technology (KAUST), Thuwal 23955-6900, Kingdom of Saudi Arabia

[2]Computational Bioscience Research Center, King Abdullah University of Science and Technology (KAUST), Thuwal 23955-6900, Kingdom of Saudi Arabia

(This article belongs to the *Special Issue: Related to 3D printing technology and materials*)

Abstract

Three-dimensional (3D) bioprinting systems, which are the prominent tools for biofabrication, should evolve around the cutting-edge technologies of tissue engineering. This is the case with organoid technology, which requires a plethora of new materials to evolve, including extracellular matrices with specific mechanical and biochemical properties. For a bioprinting system to facilitate organoid growth, it must be able to recreate an organ-like environment within the 3D construct. In this study, a well-established, self-assembling peptide system was employed to generate a laminin-like bioink to provide signals of cell adhesion and lumen formation in cancer stem cells. One bioink formulation led to the formation of lumen with outperforming characteristics, which showed good stability of the printed construct.

Keywords: Laminin; Biofunctional bioink; Self-assembling peptide; Organoid; IKVAV

†These authors contributed equally to this work.

***Corresponding author:**
Charlotte A. E. Hauser
(charlotte.hauser@kaust.edu.sa)

Citation: Pérez-Pedroza R, Al-Jalih F, Xu J, *et al.*, 2023, Fabrication of lumen-forming colorectal cancer organoids using a newly designed laminin-derived bioink. *Int J Bioprint*, 9(1): 633. https://doi.org/10.18063/ijb.v9i1.633

Received: July 21, 2022
Accepted: August 05, 2022
Published Online: November 4, 2022

1. Introduction

Three-dimensional (3D) bioprinting is widely recognized as one of the most prominent enabling technologies for tissue biofabrication. In view of the extensive use and versatility of 3D bioprinting, it is important that these systems evolve around the cutting-edge technologies of tissue engineering. This is the case with organoid technology. Organoids are currently one of the most studied *in vitro* systems for tissue engineering approaches. These self-organizing cellular structures can recapitulate the diversity of cell lineages and functionalization of human tissues, beginning from single pluripotent cells[1]. Organoids are suitable for studying and investigating organ behavior and function, as they are able to recapitulate cellular metabolism[2], epigenomic signatures[3], gene expression[4], and even developmental programming[5] from the original tissue. At present, particularly in this fascinating period of time with personalized treatment, big data management, and fast-rising innovative technologies, there is a high demand for new methods that can combine the benefits of organoid models with the precision of 3D bioprinting[6].

It is widely known that organoids can only be fabricated within 3D matrices that mimic the mechanical and biochemical properties of extracellular matrix (ECM); to this end, researchers mostly depend on naturally derived hydrogels, such as decellularized ECM, laminin, fibrinogen, and collagen[7,8]. For instance, a gelatin methacryloyl (GelMA)-based bioresin was used in a volumetric 3D printer to generate a construct that contains liver organoids to be deployed as metabolic "biofactories"[9]. The bioresin had to be formulated together with a refractive index matching compound in order to tune the printing performance of GelMA. Cell polarization and hepatic differentiation were observed after 10 days of culture. On the other hand, researchers have generated vascularized neural organoids by using commercial gelatin/fibrinogen-based bioinks[10]. Interestingly, the reported method allows for the simultaneous differentiation of vascular endothelium and neurons from pluripotent cell lines while retaining their identity during co-culture. From the coupling of this new method with multi-material bioprinting to produce integer vascularized organoids, researchers were able to reproduce the geometry of a human dorsal forebrain coronal section.

Despite the positive outcomes of these techniques, the use of these biomaterials carries several disadvantages, such as immunogenicity, batch-to-batch variability, xenogenic material, and presence of unwanted growth factors[11]. Moreover, these materials lack mechanical tunability and have shown poor performance as bioinks, for which they need to be chemically modified to be light-reactive. Similarly, supplemented synthetic materials have shown promising discovery as tunable matrices for organoids[12]. Still, all these options require ultraviolet (UV) crosslinking, which introduces risk to the embedded cellular structures. In this work, the biofunctionalization of a known self-assembling peptide (SAP) was proposed to design a novel laminin-like bioink.

Self-assembling peptides are amphiphilic molecules that can spontaneously aggregate into complex 3D structures such as nanofibers[13]. Given their similarities to ECMs, nanofiber-forming SAPs have shown to be an alternative for 3D cell culture. SAPs, developed by the Hauser Group, have shown to be biocompatible, biodegradable, and non-immunogenic; additionally, they can gelate to fibrillar hydrogels under controlled physiological conditions and specific concentrations[14-18]. Moreover, SAPs provide compositional control and simplicity in synthesis. These SAPs can be used as bioinks in a dual extrusion setting to generate 3D constructs of up to 4 cm in height[14]. In order to provide cues for the growth of colorectal cancer cells, we supported a previously developed SAP sequence (IIFK) with laminin-derived IKVAV motif and a newly synthesized peptide containing both IIFK and IKVAV moieties to obtain a biofunctional IKVAV-derived peptide (IDP) sequence[19,20].

We expect that the interruption of the polarity gradient of the tetrapeptide might adversely affect the assembly, thereby reducing the mechanical properties of the hydrogel. In order to overcome this, we hypothesize that by mixing a parent SAP together with its biofunctional version, we can create a backbone to sustain the biochemical cues in the matrix. A similar strategy has been used before, where two self-assembling peptides derived from RADA16 were biofunctionalized with IKVAV and arginylglycylaspartic acid (RGD) motifs[21]. This approach used oppositely charged RADA peptides to induce self-assembly. A molecular model, in which a non-biofunctional RADA16 "core" stabilizes the random coils formed by the functional motifs, was proposed. Moreover, IKVAV is known as a self-assembling peptide itself, capable of forming nanofibers that promote cell growth (in particular, neuron growth and development)[22,23].

The proposed strategy would guarantee a constant concentration of a small molecule of interest in the matrix, even during cell proliferation, whereas a free molecule would diffuse, and its effect in cells would diminish over time. Furthermore, the use of a biofunctional peptide will reassure a homogeneous distribution of the biofunctional signal in 3D constructs. With regard to the biofunctional part of this new peptide, we presume that the introduction of a laminin-derived motif (IKVAV, active site in LMα1) into a self-assembling peptide will have an effect on cell behavior similar to that of the motif itself.

Given that colorectal organoids secrete laminin in order to maintain structural integrity[24], we speculate that this bioactive peptide can be employed as an alternative material for organoid-like structures in bioprinted scaffolds. In addition, laminin receptors are highly expressed in colorectal cancer cells[25]. By introducing the presence of a cell-interacting motif, like laminin-111, we expect to obtain a minimalist matrix that mimics the ECM characteristics that allow organoid formation.

This biofunctional SAP will allow us to retain the mechanical properties[14,26-29] as well as the tunability and printability of our previously reported SAP, while incorporating a known cue for cell–matrix interactions. Here, we investigated the effect of this motif on cell proliferation and lumen formation as an early organoid formation signal. We also evaluated the bioprintability of this modified tetrapeptide hydrogel by investigating the cell viability and proliferation of a printed construct with cells for possible tissue engineering applications. Both manual and bioprinted construct containing IDP demonstrated clear advantages, particularly in organoid

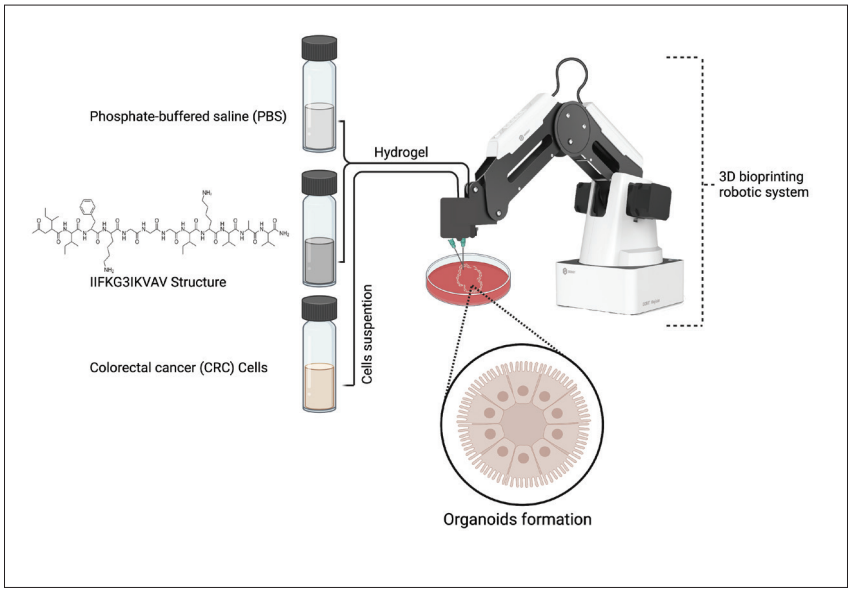

Figure 1. A graphical abstract of using IDP for 3D bioprinting of colorectal cancer cells by an in-house bioprinting setup.

lumen formation, over the single peptide IIFK and the control Matrigel (a graphical abstract of the work is shown in Figure 1).

2. Materials and methods

2.1. Peptide synthesis

IIFK (Ac-Ile-Ile-Phe-Lys-NH2), IKVAV (Ac-Ile-Lys-Val-Ala-Val-NH2), and IDP (Ac-Ile-Ile-Phe-Lys-Gly-Gly-Gly- Ile-Lys-Val-Ala-Val-NH2) were synthesized by Fmoc-based solid-phase peptide synthesis (SPPS). The peptides were purified by high-pressure liquid chromatography-mass spectroscopy (HPLC-MS). The peptide mass and structure were confirmed by mass spectrometry (MS) and nuclear magnetic resonance (NMR) spectra analysis (Figure S1).

2.2. Hydrogel formation

Aqueous peptide solutions were prepared by dissolving lyophilized peptide powders in Milli-Q water and vortexing as well as sonicating for 5 min until fully dissolved. The hydrogel formation was initiated by adding 10× phosphate-buffered saline (PBS) to the aqueous peptide solution to reach a final concentration of 9:1 peptide solution to PBS. In order to find the critical gelation concentration, vial inversion tests were performed on each peptide using different concentrations.

2.3. Mechanical properties analysis of hydrogel

The mechanical properties of the peptide hydrogels were determined by performing an oscillatory rheological test using TA Ares G2 rheometer equipped with 8 mm parallel-plate geometry and a gap distance of 1.5 mm at 22°C. Hydrogels were prepared inside a 9 mm inner diameter glass ring treated with Sigmacote by first dissolving them in Milli-Q water and then adding 10× PBS to a final concentration of 1× PBS. Six replicates with a volume of 200 µL were prepared 21 h prior to measurements.

2.4. Proton nuclear magnetic resonance (^{1}H NMR)

Peptides were exposed to UV sterilization and subsequently diluted in dimethyl sulfoxide-d6. Spectra were acquired on a Bruker Avance III 600 MHz NMR spectrometer equipped with a 5 mm Z-gradient SmartProbe BB(F)-H-D (Bruker BioSpin, Rheinstetten, Germany).

2.5. Atomic force microscopy (AFM) imaging

JPK Nanowizard 3 AFM mounted on Olympus IX73 optical microscope was user to measure the sample in air. AFM probes (AC240TS-R3 from Olympus) with a nominal resonance frequency of about 70 kHz were used in tapping mode. The samples were dissolved in Milli-Q water to a final concentration of 8 mM by vortexing. The solution was left at room temperature for 24 h; thereafter, 20 µL was pipetted on a freshly cleaved mica sheet and immediately rinsed 3 times with 1 mL of Milli-Q water. The solution was left to dry in a vacuum chamber overnight. The AFM measurement was performed at 50% RH. Following the flattening of the AFM height channel, more than 20 orthogonal and longitudinal profiles were extracted to extrapolate the characteristic lengths of the fibers.

2.6. Scanning electron microscope (SEM) imaging

Electron microscopies were obtained from dehydrated scaffolds in an FEI Magellan 400 XHR Scanning Electron Microscope under high vacuum, with an accelerating

voltage of 3.00 kV. The SEM sample was prepared by transferring a cell-laden peptide hydrogel onto a glass coverslip. The gel was then dehydrated by immersing it in a series of ethanol solutions of increasing concentrations. The dehydrated gels were then dried in the Automated Critical Point Dryer. The dried samples were sputter coated with 5 nm iridium (Ir) before imaging.

2.7. Circular dichroism spectroscopy

Circular dichroism (CD) spectra were acquired at ambient temperature (25°C) using the Aviv 430 spectrometer (Aviv Biomedical Inc., Lakewood, NJ, USA). Nitrogen gas was used to keep the oxygen level around 5 ppm. Rectangular quartz cuvettes with optical path length of 0.1 mm (0.01 mm when the dynode value was above 500 V) were used. Data acquisition was performed at 1 nm steps, scanning the wavelength (λ) from 300 nm to 190 nm with a spectral bandwidth of 1.0 nm. The CD signals were further normalized to the molar ellipticity value. Aviv 35 CD instrument and OriginPro 2017 64-bit software were used for data collection and processing, respectively. The CD spectra were smoothed to remove the background noise, without changing the signal. The samples were freshly synthesized and prepared by dissolving different concentrations in Milli-Q water.

2.8. Culture of colorectal cancer stem cells and cell seeding in 3D hydrogel

Commercial colorectal carcinoma-derived cell line SW1222 was used. Cells were maintained in a fresh medium, comprising of Iscove's Modified Dulbecco's Medium (IMDM) (Gibco), supplemented with 1% penicillin and 10% fetal bovine serum (FBS), in a carbon dioxide (CO_2) incubator at 37°C with 5% CO_2. The culture media were changed every 3 days. Cells at passages 8 to 10 were used. Cells were split using trypsin, and single cells were obtained by running the cells through a 40 μm strainer. Cells were mixed with PBS and loaded to the pre-gel peptide solutions. Before seeding the cells, the peptides were sterilized by UV for 1 h for 3D hydrogel culture. For cell viability and proliferation assays, 96-well plate was used to form 100 μL of 3D hydrogel from the peptide solution (8 mM, 10 mM, and 12 mM of IIFK, IDP, and IKVAV each, and a mix of IIFK with IDP at a 5:1 ratio) with 7000 cells suspended in 2× PBS. In preparing for cytoskeletal staining, the same method was used to form a droplet construct in a 24-well plate, with a total volume of 15 μL and 1000 cells. Matrigel and 2D cell culture were used as positive controls. Media were added to each well on culture plates.

2.9. Adhesion assays

Upon adding 50 μL of peptide and 50 μL of 2× PBS, a thin layer of hydrogel was formed on the surface of a 6-well plate. The peptide was left to incubate at room temperature for 15 min. SW1222 cells were seeded on top of the wells at a density of 40,000 cells/cm^2 and left to incubate at 37°C, under 5% CO_2. After 90 min, half of the well plates were fixed with formaldehyde 4% for 30 min. The other half was exposed to mechanical stress to induce cell detachment. Cells were fixed as mentioned earlier, and all well plates were stained for 10 min with 4′,6-diamidino-2-phenylindole (DAPI) for cell quantification under the microscope[30].

2.10. Cell viability and proliferation assessment

At each time point of culture, the viability of colorectal cancer (CRC) cells in the 3D hydrogel scaffolds was determined by LIVE/DEAD Viability/Cytotoxicity Kit (Invitrogen, Thermo Fisher). The staining solution was prepared with 8 μM ethidium homodimer-1 (EthD-1) and 8 μM calcein AM in 1× PBS. The cell samples were washed 3 times with 1× PBS and then incubated in the staining solution for 45 min. After staining, the staining solution was removed, and the samples were washed 3 times with 1× PBS. ZEISS Axio Vert fluorescence microscope was used to view the cells. In order to determine the proliferation rate of cells, the CellTiter-Glo luminescent viability assay was used. One hundred microliter (equivalent to culture medium used with samples) of CellTiter-Glo reagent was added into each well and mixed thoroughly. The samples were incubated for 25 min at room temperature. A PHERAstar FS plate reader was used to read the plates.

2.11. Cytoskeletal staining

Immunostaining was performed using Rhodamine phalloidin (Invitrogen, Thermo Fisher) for F-actin staining. After fixing the cells with 4% paraformaldehyde (PFA) for 30 min, cells were permeabilized with 0.2% Triton X-100 in 1× PBS for 1 h. The permeabilized cells were then incubated in a blocking buffer solution, containing 1% bovine serum albumin in 1× PBS, and left overnight. Rhodamine phalloidin (1:40) was added to the cells and left for 24 h. Thereafter, the cells were washed with 1× PBS, incubated in DAPI for 10 min, and then washed with 1× PBS. Finally, the cells were imaged using a laser scanning confocal microscope (Zeiss LSM 710 inverted confocal microscope).

2.12. Image processing

By measuring the diameter of the spots, and assuming that the shape is circular for comparison, ImageJ image analysis software was used to measure the lumen size.

2.13. 3D bioprinting and construct assessment

An in-house-developed printing system was used to test the printability of each peptide hydrogel. The robotic 3D printing system consists of microfluidic pumps, a robotic arm with five degrees of freedom, and a dual-coaxial nozzle. Three microfluidic pumps were used in this system: one for the peptide, one for PBS, and the other for the cells. The

pumps' system allows for a specific flow rate for each solution, thus resulting in a more consistent printed structure. The DOBOT Magician robotic arm with a modified head was used to mount the in-house-designed and -fabricated nozzle. The nozzle used was custom designed to have three inlets and one outlet with a 0.5 mm inner diameter. Two of the inlets are for the peptide solution and 1× PBS to merge and form the hydrogel, and the third is for cell dispensing. Flow rates of 50 µL/min, 25 µL/min, and 15 µL/min were used for the peptide solution, PBS, and cells, respectively. Printing files were designed with SOLIDWORKS and transferred to Repetier-Host to obtain the G-code for 3D printing with the robotic arm.

2.14. Statistical analysis

Statistical analysis was performed by using the one-way analysis of variance (ANOVA) and two-way ANOVA tests. Significance was evaluated using Fisher's LSD and considered to be statistically relevant below $P = 0.05$ (*) and $P = 0.01$ (**) using OriginPro (Origin 2022b version 9.9).

3. Results

3.1. Physicochemical characterization of laminin-like biofunctional peptide

The self-assembling peptide IIFK was considered for use in this study based on the previously reported positive effect on cell expansion[14]. IIFK is composed of a hydrophobic tail from nonpolar amino acids (Ile, I and Phe, F) and a positively charged amino acid (Lys, K) at the C-terminal, which gives this peptide its amphiphilic nature. This amphiphilic property enables the self-assembly of IIFK into ordered supramolecular nanofibers. A combination of the tetrapeptide IIFK and the IKVAV motif with a linker was rationally designed and investigated for its gelation capability (chemical structures in Figure 2A). Inverted vial tests were performed to monitor the critical gelation concentration (CGC) and gelation time for IIFK, IKVAV, and the new IKVAV-derived peptide (IDP), respectively (Figure 2B). The gelation results (Figure 2B, Figure S2) showed that IDP has a CGC of 2 mg/mL, while in combination with IDP (1:1), it increases to 3 mg/mL. The gelation time of IDP at CGC is 20 s, while the mixture decreases its gelation time to 10 min.

Furthermore, SEM micrographs and AFM topography performed on the three peptides showed a nanofibrous morphology (Figure 2C and D). Table 1 shows the characteristic AFM lengths of the fibers formed by IIFK, G3, and the mixture of the two. We can observe how the morphology of the fibers from IIFK and IIFK:IDP (1:1) Mix resembles each other more compared to the fibers from IDP. This sort of self-assembly into fibrous structure is advantageous as it has the ability to form hydrogels and therefore a suitable environment for cellular growth. Extracellular matrix is characterized by the presence of collagen, which forms an intricate network of fibers that support cell growth[18,28,29]. Both the IIFK and IKVAV motifs are amphiphilic in nature and have been reported to be able to form fibers in solution[31,32]. Interestingly, longer IDP peptide displays self-assembling characteristics into nanofibers as well, which may be attributed to the amphiphilic nature of IKVAV, along with the gradient of hydrophobicity of peptide IIFK.

In addition, we investigated the secondary structure of the two peptides and the peptide mixture by using CD spectroscopy (Figure 2E, Figure S3). The CD spectra of IIFK showed a gradual structural transition from a disordered to a partially ordered structure at low concentrations. The spectrum at 1 mg/mL showed a negative peak around 195 nm, which is characteristic of random coil structure, while the spectrum at 4 mg/mL showed a positive peak around 195 nm and a negative peak around 220 nm, which is typical of β-sheet. A transition between the two structures is evident at 3 mg/mL. A gradual structural transition from a disordered to an ordered structure was observed for IDP at 1 mg/mL, 2 mg/mL, and 3 mg/mL; a similar transition was observed for IIFK:IDP (1:1 molarity ratio) at 1 mg/mL, 3 mg/mL, and 4 mg/mL. The observed transition suggests a structural transformation in the peptide from random coil to β-sheet since the peak that is around 195 nm (π π^*) is characteristic of random coil structure, while the maximum around 200 nm (π π^*) and the minimum around 220 nm (n π^*), seen in both IDP and peptide mixture at the highest concentrations, are typical of antiparallel β-sheet[33]. Therefore, we can appreciate how the combination of IIFK and IDP provides a different secondary structure milieu compared to individual elements.

We proceeded with the analysis of the rheological properties of these materials. Based on the time sweep test performed, we confirmed that these peptides are able to form gels with tunable mechanical properties. The stiffness of different concentrations of IIFK and the combination of IIFK and IDP was examined by measuring the storage modulus (G'). The mechanical stiffness of these two hydrogels increases as the final concentration increases (Figure 2F, Figure S4). When compared with each other, IIFK by itself had higher G' values than when it is combined with the modified IIFK. The rigidity of both hydrogels was within the rigidity range that supports continuing multipotency maintenance[15,32] and bioprinting[14].

3.2. Cell viability and proliferation of CRC cells in biofunctional hydrogel scaffold

A screen study was performed to investigate the biocompatibility of the different peptides and their effect

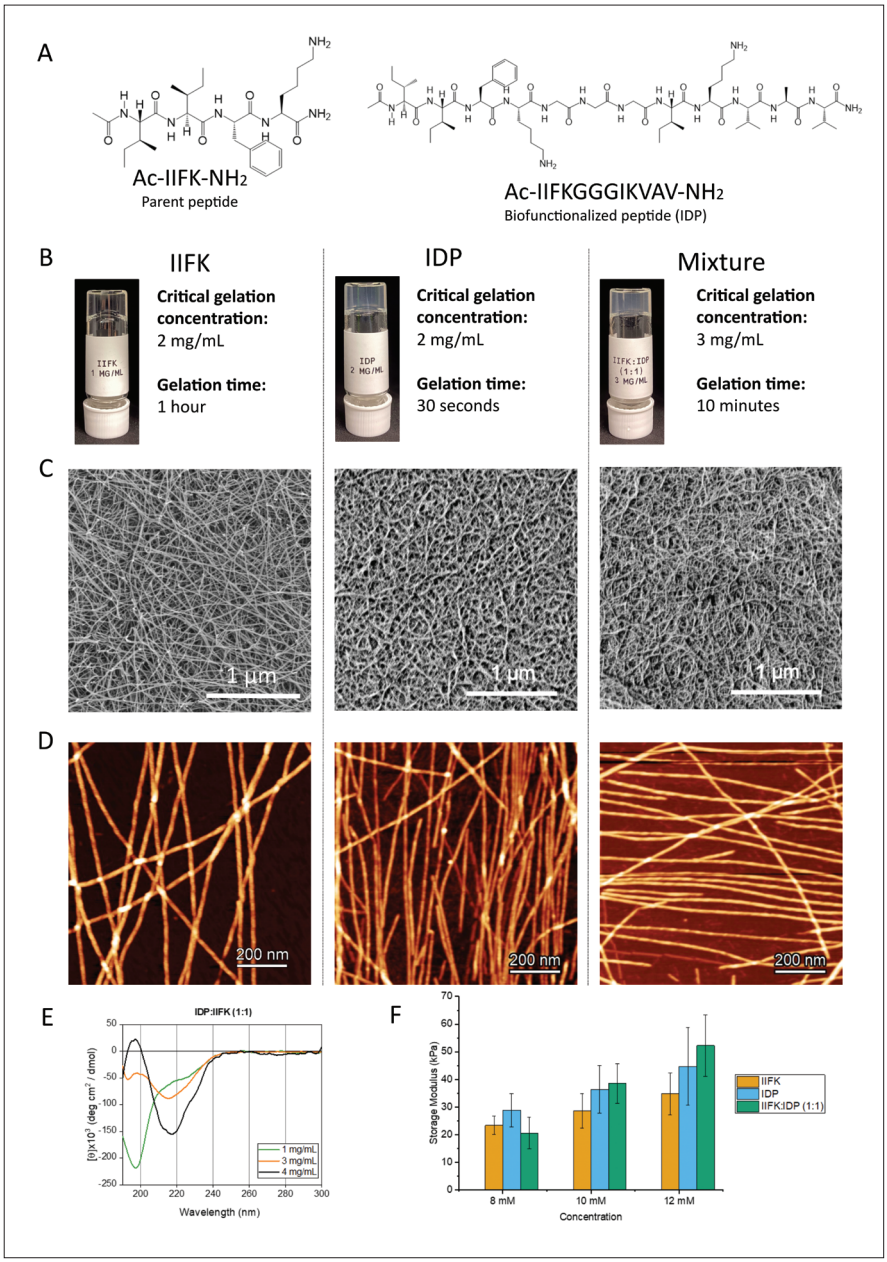

Figure 2. Physicochemical characterization of IIFK, IDP, and IIFK:IDP (1:1) mixture. (A) Chemical structure of the parent peptide IIFK and biofunctional peptide IDP. (B) Inverted vial test results for CGC and gelation time. IDP generates a translucent gel that gelates with a higher CGC compared to the parent peptide IIFK. The IIFK:IDP (1:1) mixture shows a higher CGC and higher gelation time for all 3. (C) SEM micrographs of IIFK, IDP, and IIFK:IDP. (D) AFM height topography images for the gelated peptides at 8 mM. (E) CD spectroscopy of the IIFK:IDP mixture at different concentrations. (F) Stiffness of the gelated peptides at varying concentrations measured by rheological analyses.

Table 1. Characteristic lengths of the fibers formed by the three peptides IIFK, IDP, and mixture of both (Mix) according to AFM topography

Peptide	Height (nm)	Periodicity (nm)
IIFK	7.23 ± 0.76	55.58 ± 1.93
IDP	4.38 ± 1.05	31.40 ± 9.76
Mix	5.92 ± 0.66	56.31 ± 9.08

on cell viability at 3 mg/mL (CGC of the IIFK:IDP (1:1) Mix) and 4.5 mg/mL (8 mM). Additionally, we performed proliferation assays to estimate the growth of CRC cells in the peptide scaffolds by measuring resazurin cellular reduction at days 1, 4, and 7 of culture (Figure 3). The laminin-based peptide IDP showed promising results. When compared to Matrigel, no treatment presented a significant decrease in terms of viability and cell proliferation ($P < 0.01$, comparison of means by Fishers LSD). Interestingly, we find that, by day 7, cells proliferate better in our parent peptide at the lowest concentration and in 2D. Compared with the Matrigel control, the rest of the treatments (IIFK at 4.5 mg/mL, and IDP and Mix at both concentrations) have similar viability and proliferation profile during the 7 days of culture. Nevertheless, the high percentage of cell viability indicates that there was no cytotoxic effect throughout the culture time (Figure 3A). Compared with Matrigel control, comparable proliferation rates were observed in IIFK and IIFK:IDP peptide mixtures at higher concentration scaffolds (4.5 mg/mL).

3.3. Adhesion of CRC cells to biofunctionalized scaffold

In order to evaluate the effect of the biofunctionalized peptide in cell adherence, we quantified the change of cell adherence on the surface of IIFK, IKVAV, IDP, and the IIFK:IDP (1:1) and (10:1) Mix at 8 mM concentration. We evaluated the concentration effect of IDP by establishing one mixture with high concentration of IDP (1:1) and another mixture with low concentration of IDP (10:1) in order to compare the effect of the presence of IIFK fibers and IKVAV motif. We quantified the area covered with cells before and after exerting mechanical stress in the surface on the hydrogel to induce separation of cells from the hydrogel surface. The results are shown in Figure 4.

Cells show significant detachment from IKVAV and IIFK:IDP (10:1) scaffolds. Interestingly, the non-biofunctionalized peptide IIFK had a lower initial retention of the seeded cells (18% of the surface area) but showed a high index of cell retention after the mechanical stress was applied (77% of the seeded population was retained). However, the IKVAV scaffold induced an increase in cell

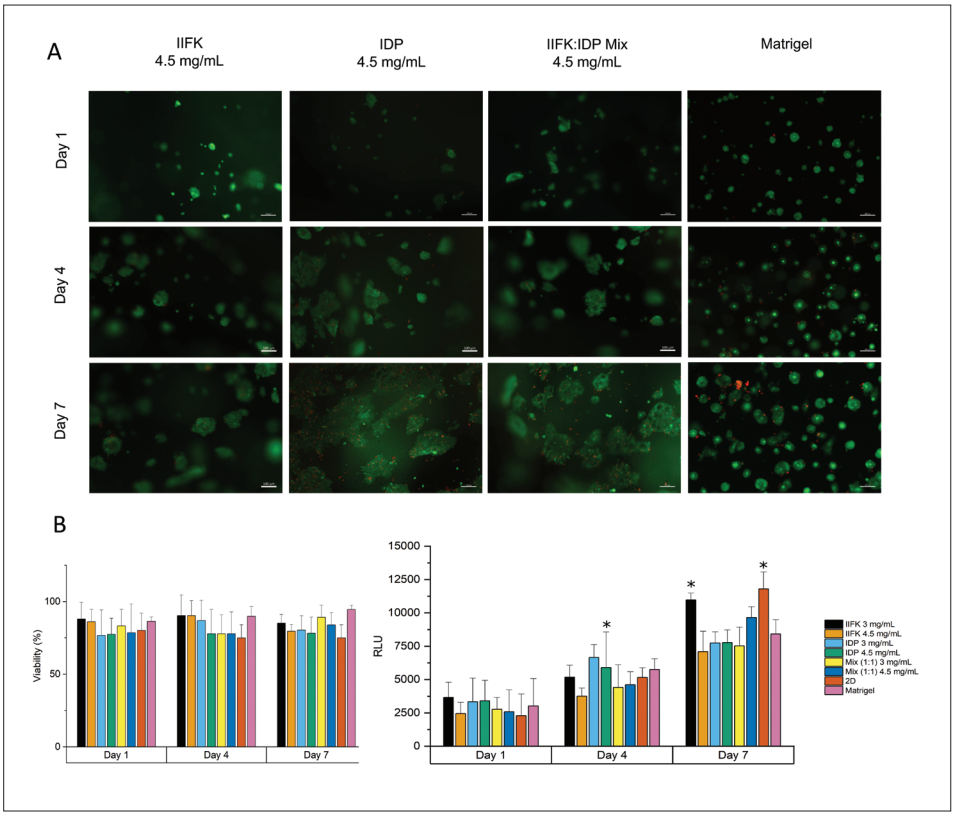

Figure 3. Influence of different peptide hydrogels on cell viability. (A) Cell viability staining images of CRC cells in IIFK, IKVAV, IDP, and IIFK:IDP after 1, 4, and 7 days of culture. Calcein AM (live cells, green) and ethidium homodimer-1 (dead cells, red) were used to stain the cells. Matrigel was used as a positive control. Scale bar is 100 μm. (B) (left) Cell viability percentages obtained using a fluorescence plate reader; (right) cell proliferation assessment in different hydrogel scaffolds with different concentrations in comparison to 2D culture. Proliferation assay after 1 and 7 days of culture. * and ** represent statistically different results at $P < 0.05$ and $P < 0.01$.

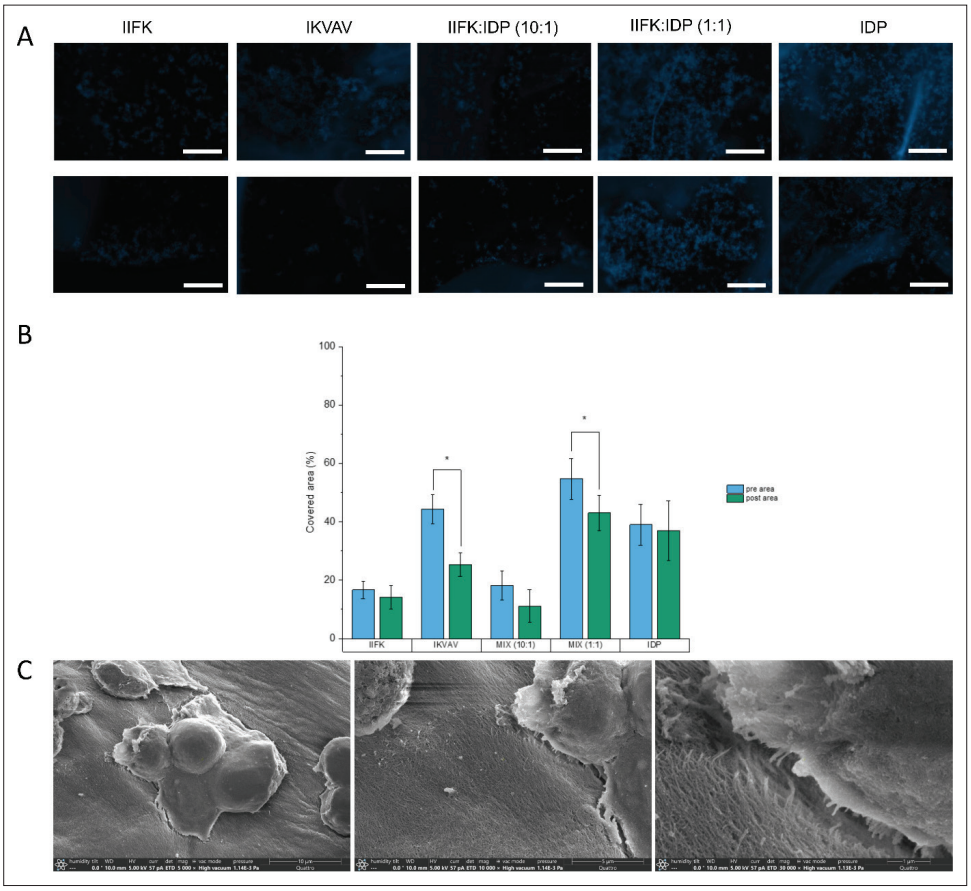

Figure 4. Cell adhesion assays with varying SAP formulations at 8 mM. (A) Before (upper) and after (lower) mechanical detachment induction of SW1222 cells on the parent peptide (IIFK), laminin peptide (IKVAV), IKVAV-derived peptide (IDP), and an IIFK:IDP (1:1) Mix. Scale bars are 100 μm. (B) Quantification of cells attached to the matrix before and after mechanical stress was applied. (C) SEM images of SW1222 cells cultured overnight in IIFK:IDP (1:1) at 8 mM, showing cell–matrix interactions. * represents statistically different results at $P < 0.05$.

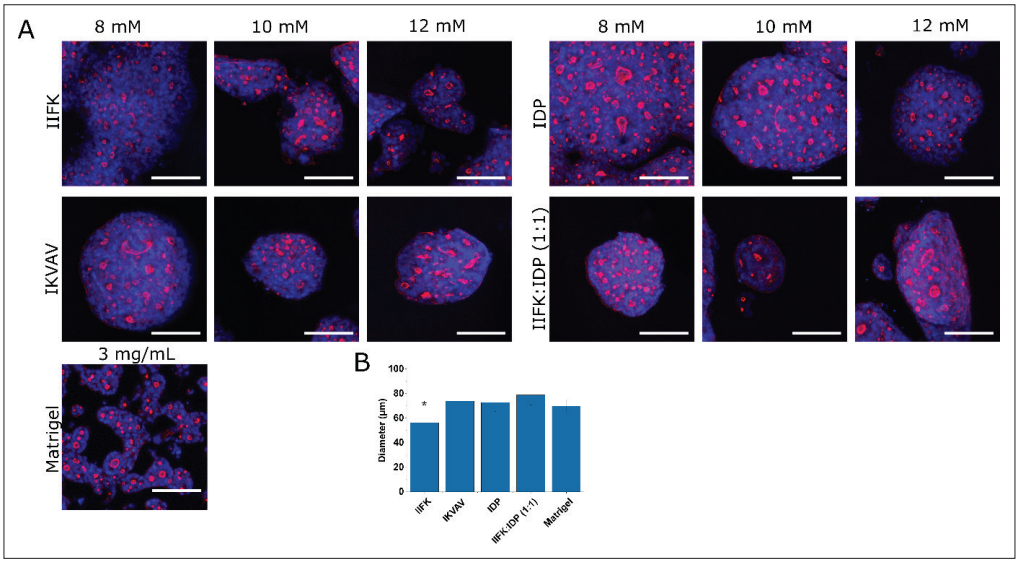

Figure 5. Characterization of CRC colonies in hydrogel scaffolds. (A) Rhodamine phalloidin was used to stain F-actin (red), and DAPI was used to stain the nucleus (blue). Assessment of morphology in hydrogel scaffolds with different concentrations: 8 mM, 10 mM, and 12 mM. Scale bar is 100 μm. (B) Comparison of lumen diameters of organoids in different peptides at day 7. * represents statistically different results at $P < 0.05$.

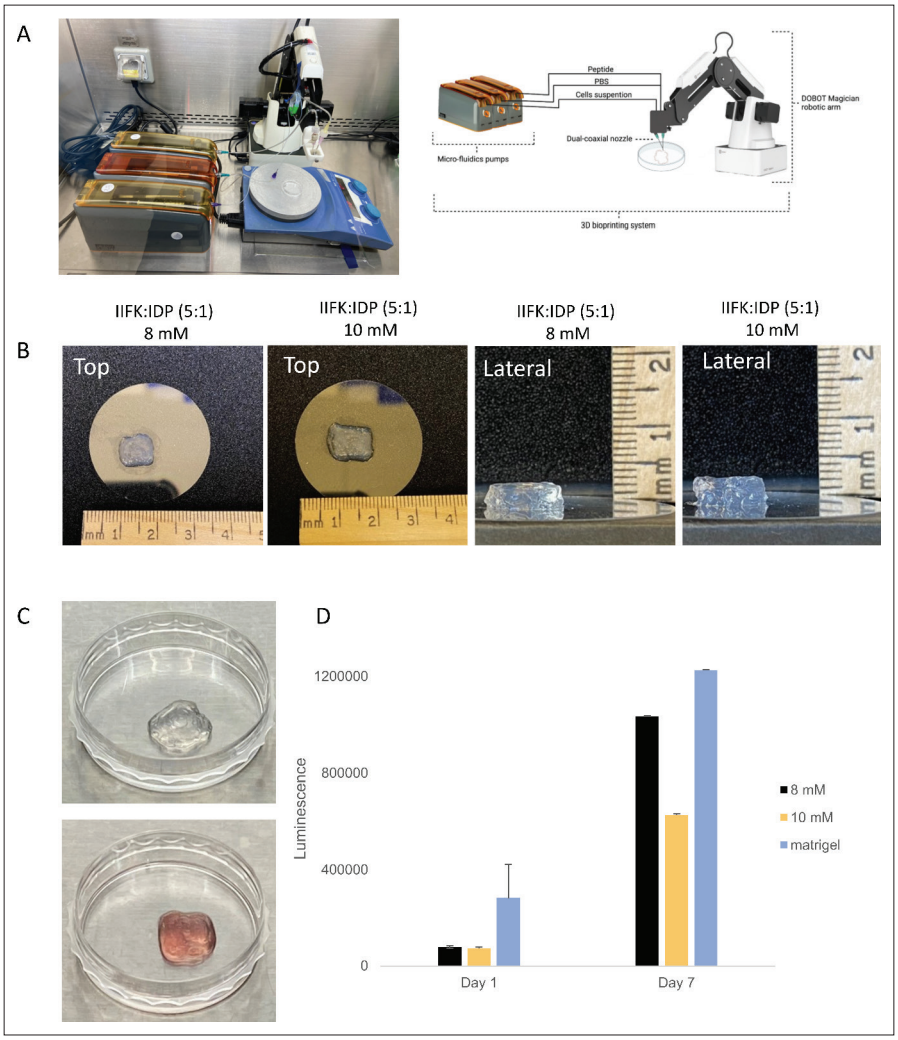

Figure 6. Three-dimensional printed construct using IIFK:IDP hydrogel. (A) In-house bioprinting setup with robotic arm setup. (B) Top and side views of printed construct of IIFK:IDP (5:1) at 8 mM and 10 mM. (C) Printed constructs at days 1 and 7 of bioprinting of IIFK:IDP (5:1) at 8 mM. (D) Bioprintability assessment by cell proliferation assay in the IIFK:IDP construct after 1 and 7 days of 3D bioprinting and culture.

adherence after cell seeding (44% of the surface area) but showed a significant reduction of cell population after mechanical stress was applied (57% of the seeded population was retained). The IIFK:IDP mixtures showed two different behaviors. The one with a high concentration of IDP (1:1) resembled that of the IKVAV scaffold, while the one with high IIFK concentration (10:1) showed a closer performance to that of IIFK. Incidentally, the IDP scaffold showed high cell retention after cell seeding and the application of mechanical stress. Taken together, SAP hydrogels may facilitate physical/mechanical retention of cells in the fiber network, while IDP and IKVAV may trigger cell adhesion through integrin binding. SEM images of cells cultured in IIFK:IDP (1:1) at 8 mM were captured to observe the cell–matrix interactions formed after one day of culture (Figure 4C).

3.4. Characterization of CRC cells in scaffolds

In order to determine whether our peptide scaffolds contribute to the initial organization of cells into organoids, single CRC cells were embedded into each peptide, and the F-actin cytoskeleton and the morphology of cells were imaged with confocal fluorescence at days 4 and 7 to monitor lumen formation. Moreover, we evaluated the formation of lumen across different concentrations of peptides and compared it to lumen formed within cells cultured in Matrigel (Figure 5). Morphology of the luminal structures across the different peptides varied as we observed a more ordered configuration of cells in the biofunctionalized and IKVAV peptides. The concentrations used did not play a key role as no significant difference was observed in lumen formation (Figure 5A, Figure S5). Figure 5B shows the difference in the diameter of lumen

area in different peptide hydrogels, assuming for simplicity that the lumen is circular in shape. Larger lumens were observed in peptides containing IKVAV and IKVAV alone when compared to IIFK. Lumen formation in IIFK:IDP at different layers in 3D was also observed (Video clips S1–4).

3.5. Characterization of 3D bioprinted construct

Based on the results of the mechanical properties, cell viability, proliferation, and lumen formation of CRC cells in different self-assembling peptide hydrogels, the mixed peptide consisting of IIFK and IDP at final concentration of 8 mM and 10 mM with 5 to 1 ratio was used for 3D bioprinting. These concentrations were selected based on observations that a higher concentration of peptide is needed to produce a performant scaffold in 3D bioprinting[14]. Cell proliferation in the printed constructs was assessed at days 1 and 7 of culture. Effective cell proliferation was observed with both concentrations of peptide as the ATP released increased with time of culture. Higher proliferation rates were observed when 8 mM concentration of peptides was used and if compared to Matrigel (Figure 6).

4. Discussion

Ultrashort self-assembling peptide IIFK in combination with IKVAV was used as a hydrogel scaffold to grow lumen-containing colonies from CRC cells. This allows for native ECM mimicking and offers a 3D environment for cells. In order to manipulate the environment to meet the cells' needs, physical and chemical properties can be controlled by modifying the peptide sequence[34] to include biofunctional motifs, such as IKVAV. IKVAV is one of the active sites present in laminin chain α1 (LMα1) and highly expressed in the invasive phenotype of colon carcinoma[25]. Previous studies have shown that an increase in concentration of IKVAV peptide or laminin-111 would increase colonization rates of colon cancer into other organs[35], presumably by the mediation of tumorigenesis by LMα1. Moreover, it has been widely accepted that the IKVAV motif is recognized by integrins α3β1 and α6β1. Integrin α3β1 is required to maintain cell–cell interactions that give rise to a normal epithelial morphology[36]. The design of a novel, minimalistic, laminin-like SAP scaffold is important as smart scaffold to provide biochemical cues to cellular constructs, in order to precisely recreate the extracellular environment of native tissues; for instance, in this case, colorectal cancer tumor tissue. These findings provide an indication of the effective preparation of a modified ultrashort, self-assembling peptide hydrogel that can support CRC cells' proliferation and organoids' formation. In the current research, we investigated the effect of IKVAV on our previously developed tetrapeptide IIFK when used as a scaffold for CRC cells and compared the results to when single peptides were used.

The gelation and mechanical properties of the new IDP peptide and its combination with the parent peptide were analyzed using inverted vial test and rheological measurements. The parent peptide (IIFK) is known to have a CGC of 1 mg/mL so variation in gelation time is expected as the aggregation may be modified by the linker and the IKVAV part of the IDP sequence. Interestingly, the CGC of the IDP and IIFK (1:1) mixture and the gelation time increased compared to non-mixed peptides. This might be attributed to the fact that IDP and IIFK, having two different aggregation mechanisms, tend to compete when both monomers are present in the pre-gel solution.

One key feature of this combination is its tunable stiffness, which provides mechanically dynamic matrices[37]. We tested the effect of three different concentrations, which consequently altered the stiffness of the hydrogels, cell proliferation, and organoid formation. We found that the novel IDP peptide and its mixture with parent peptide IIFK have positive outcomes, in terms of both cell viability and proliferation. In fact, the culture of SW1222 cells within the newly designed IDP peptide scaffold and the IIFK:IDP mixtures at both concentrations (3.0 and 4.5 mg/mL) showed comparable viability profile and proliferation rates compared to Matrigel, which is the gold standard for organoid culture. It is important to note that other research[38] has suggested the possibility of IKVAV motif inducing cellular death in human intestinal organoids. However, this phenomenon was not observed in our study based on the cell viability and proliferation results. Finally, we used an established adhesion assay[30] to evaluate the effect of the biofunctional motif in the IDP peptide. We demonstrated that the laminin motif was readily available for cell binding in the IIFK:IDP (1:1) mixture as well as the single IDP scaffold.

Confocal fluorescence microscopy was also used to investigate cell morphology and their arrangement. Improved organoid formation and increased lumen area were observed across the different peptides that contained the IKVAV motif. The stiffness of the hydrogels did not play a key role as no significant difference was observed in organoids and lumen formation in the different concentrations tested. The morphology of organoid-like colonies across the different peptides varied as polarized cell configurations of organoids were detected in the modified peptides and IKVAV. This indicates that IKVAV may have a positive effect on colonies development and enhancing lumen volume when used in minimalistic matrices.

We subsequently investigated the bioprintability of this modified peptide hydrogel. A 3D construct was printed, followed by cell proliferation investigation. The printed

structure of 0.5 cm in height maintained its original shape even after more than 7 days post printing. We also found that the cells had a comparable proliferation rate to that in Matrigel when low concentration was used. This provides evidence that this modified peptide hydrogel can be a promising bioink based on synthetic material that provides a suitable, bioprintable, and biocompatible scaffold, which mimics the ECM from functional tissues, and in which cells can grow and proliferate. Therefore, this hybrid peptide can be a potential cost-effective, ECM-mimicking bioink that maintains the integrity of cells in the printed constructs.

5. Conclusion

This study provides valuable insights on the effect and performance of IKVAV motif when used in combination with the ultrashort peptide IIFK as a bioink with CRC cells. Three-dimensional constructs that positively affect cell viability can be effectively printed by utilizing the IIFK peptide that has been functionalized with IKVAV. Confocal microscopy showed signs of improved lumen formation when cells were cultured in the 3D environment of IIFK:IDP hydrogel scaffold. Importantly, it provides evidence that the use of IKVAV in combination with IIFK peptide successfully delivered signals to direct lumen formation, which increased the lumen area in the organoid formation of CRC cells as compared to other peptides. Moreover, the SAP constructs were successfully applied to 3D bioprinting, where they provided a suitable milieu for the growth of colorectal cancer colonies. This seminal study paves the way to the use of biofunctional peptides based on SAPs hydrogels as bioinks to provide active ECM for 3D bioprinting of CRC organoids.

Acknowledgments

The authors would like to acknowledge Hepi H. Susapto for supporting the NMR spectra analysis and general advice; Hamed I. Albalawi and Ali Aldhouki for training on 3D printing and laboratory support; Hamed I. Albalawi for designing graphical abstract; and KAUST's Bioscience and Imaging Core Labs for supporting the biological characterization and microscopy analyses.

Funding

This work was supported by KAUST baseline funding and CBRC funding.

Conflict of interest

The authors declare no conflicts of interest.

Author contributions

Conceptualization: Rosario Pérez-Pedroza, Charlotte A. E. Hauser

Data curation: Jiayi Xu, Fatimah Al-Jalih, Manola Moretti

Formal analysis: Fatimah Al-Jalih

Methodology: Rosario Pérez-Pedroza, Manola Moretti, Charlotte A. E. Hauser

Resources: Charlotte A. E. Hauser

Supervision: Rosario Pérez-Pedroza, Manola Moretti, Charlotte A. E. Hauser

Validation: Fatimah Al-Jalih

Writing – original draft: Fatimah Al-Jalih

Writing – review & editing: Rosario Pérez-Pedroza, Manola Moretti, Charlotte A. E. Hauser

References

1. Tuveson D, Clevers H, 2019, Cancer modeling meets human organoid technology. *Science*, 364(6444): 952–955.

   https://doi.org/10.1126/science.aaw6985

2. Sharick JT, Jeffery JJ, Karim MR, *et al.*, 2019, Cellular metabolic heterogeneity in vivo is recapitulated in tumor organoids. *Neoplasia*, 21(6): 615–626.

   https://doi.org/10.1016/j.neo.2019.04.004

3. Luo C, Lancaster MA, Castanon R, *et al.*, 2016, Cerebral organoids recapitulate epigenomic signatures of the human fetal brain. *Cell Rep*, 17(12): 3369–3384.

   https://doi.org/10.1016/j.celrep.2016.12.001

4. van de Wetering M, Francies HE, Francis JM, *et al.*, 2015, Prospective derivation of a living organoid biobank of colorectal cancer patients. *Cell*, 161(4): 933–945.

   https://doi.org/10.1016/j.cell.2015.03.053

5. Fair KL, Colquhoun J, Hannan NRF, 2018, Intestinal organoids for modelling intestinal development and disease. *Philos Trans R Soc Lond B Biol Sci,* 373(1750): 20170217.

   https://doi.org/10.1098/rstb.2017.0217

6. Clevers H, Tuveson DA, 2019, Organoid models for cancer research. *Annu Rev Cancer Biol,* 3(3): 223–234.

   https://doi.org/10.1146/annurev-cancerbio-030518-055702

7. Sato T, Clevers H, 2015, SnapShot: Growing organoids from stem cells. *Cell*, 161(7): 1700–1700 e1.

   https://doi.org/10.1016/j.cell.2015.06.028

8. Sato T, Stange DE, Ferrante M, *et al.*, 2011, Long-term expansion of epithelial organoids from human colon, adenoma, adenocarcinoma, and Barrett's epithelium. *Gastroenterology*, 141(5): 1762–1772.

   https://doi.org/10.1053/j.gastro.2011.07.050

9. Bernal PN, Bouwmeester M, Madrid-Wolff J, *et al.*, 2022, Volumetric bioprinting of organoids and optically tuned hydrogels to build liver-like metabolic biofactories. *Adv Mater*, 34(15): e2110054.

   https://doi.org/10.1002/adma.202110054

10. Skylar-Scott MA, Huang JY, Lu A, *et al.*, 2022, Orthogonally induced differentiation of stem cells for the programmatic patterning of vascularized organoids and bioprinted tissues. *Nat Biomed Eng*, 6: 449–462.

https://doi.org/10.1038/s41551-022-00856-8

11. Aisenbrey EA, Murphy WL, 2020, Synthetic alternatives to Matrigel. *Nat Rev Mater*, 5(7): 539–551.

https://doi.org/10.1038/s41578-020-0199-8

12. Gjorevski N, Sachs N, Manfrin A, *et al.*, 2016, Designer matrices for intestinal stem cell and organoid culture. *Nature*, 539(7630): 560–564.

https://doi.org/10.1038/nature20168

13. Pérez-Pedroza R, Ávila-Ramírez A, Khan Z, *et al.*, 2021, Supramolecular biopolymers for tissue engineering. *Adv Polym Tech*, 2021: 23.

https://doi.org/10.1155/2021/8815006

14. Susapto HH, Alhattab D, Abdelrahman S, *et al.*, 2021, Ultrashort peptide bioinks support automated printing of large-scale constructs assuring long-term survival of printed tissue constructs. *Nano Lett*, 21(7): 2719–2729.

https://doi.org/10.1021/acs.nanolett.0c04426

15. Loo Y, Chan YS, Szczerbinska I, *et al.*, 2019, A chemically well-defined, self-assembling 3D substrate for long-term culture of human pluripotent stem cells. *ACS Appl Bio Mater*, 2(4): 1406–1412.

16. Chan KH, Xue B, Robinson RC, *et al.*, 2017, Systematic moiety variations of ultrashort peptides produce profound effects on self-assembly, nanostructure formation, hydrogelation, and phase transition. *Sci Rep*, 7(1): 12897.

https://doi.org/10.1038/s41598-017-12694-9

17. Lakshmanan A, Cheong DW, Accardo A, *et al.*, 2013, Aliphatic peptides show similar self-assembly to amyloid core sequences, challenging the importance of aromatic interactions in amyloidosis. *Proc Natl Acad Sci*, 110(2): 519–524.

https://doi.org/10.1073/pnas.1217742110

18. Hauser CA, Deng R, Mishra A, *et al.*, 2011, Natural tri- to hexapeptides self-assemble in water to amyloid beta-type fiber aggregates by unexpected alpha-helical intermediate structures. *Proc Natl Acad Sci U S A*, 108(4): 1361–1366.

https://doi.org/10.1073/pnas.1014796108

19. Sordat I, Bosman FT, Dorta G, *et al.*, 1998, Differential expression of laminin-5 subunits and integrin receptors in human colorectal neoplasia. *J Pathol*, 185(1): 44–52.

https://doi.org/10.1002/(SICI)1096-9896(199805)185:1<44::AID-PATH46>3.0.CO;2-A

20. Sordat I, Rousselle P, Chaubert P, *et al.*, 2000, Tumor cell budding and laminin-5 expression in colorectal carcinoma can be modulated by the tissue micro-environment. *Int J Cancer*, 88(5): 708–717.

https://doi.org/10.1002/1097-0215(20001201)88:5<708::Aid-Ijc5>3.3.Co;2-A

21. Sun Y, Li W, Wu X, *et al.*, 2016, Functional self-assembling peptide nanofiber hydrogels designed for nerve degeneration. *ACS Appl Mater Interfaces*, 8(3): 2348–2359.

https://doi.org/10.1021/acsami.5b11473

22. Wu Y, Zheng Q, Du J, *et al.*, 2006, Self-assembled IKVAV peptide nanofibers promote adherence of PC12 cells. *J Huazhong Univ Sci Technol*, 26(5): 594–596.

https://doi.org/10.1007/s11596-006-0530-7

23. Xu H, Shao Z, Wu Y, *et al.*, 2009, Effects of self-assembled IKVAV peptide nanofibers on olfactory ensheathing cells. *Chin J Biotechnol*, 25(2): 292–298.

24. Buzzelli JN, Ouaret D, Brown G, *et al.*, 2018, Colorectal cancer liver metastases organoids retain characteristics of original tumor and acquire chemotherapy resistance. *Stem Cell Res*, 27: 109–120.

https://doi.org/https://doi.org/10.1016/j.scr.2018.01.016

25. Cioce V, Castronovo V, Shmookler BM, *et al.*, 1991, Increased expression of the laminin receptor in human colon cancer. *J Natl Cancer Inst*, 83(1): 29–36.

https://doi.org/10.1093/jnci/83.1.29

26. Seow WY, Salgado G, Lane EB, *et al.*, 2016, Transparent crosslinked ultrashort peptide hydrogel dressing with high shape-fidelity accelerates healing of full-thickness excision wounds. *Sci Rep*, 6(1): 32670.

https://doi.org/10.1038/srep32670

27. Fauchere J-L, Charton M, Kier LB, *et al.*, 1988, Amino acid side chain parameters for correlation studies in biology and pharmacology. *Int J Pept Prot Res*, 32(4): 269–278.

28. Chaudhuri O, Gu L, Klumpers D, *et al.*, 2016, Hydrogels with tunable stress relaxation regulate stem cell fate and activity. *Nat Mater*, 15(3): 326–334.

https://doi.org/10.1038/nmat4489

29. Haugh MG, Vaughan TJ, Madl CM, *et al.*, 2018, Investigating the interplay between substrate stiffness and ligand chemistry in directing mesenchymal stem cell differentiation within 3D macro-porous substrates. *Biomaterials*, 171: 23–33.

https://doi.org/10.1016/j.biomaterials.2018.04.026

30. Humphries MJ, 2009, *Cell Adhesion Assays, Extracellular Matrix Protocols*, Springer, New York City, 203–210.

31. Arthur A, Zannettino A, Gronthos S, 2009, The therapeutic applications of multipotential mesenchymal/stromal stem cells in skeletal tissue repair. *J Cell Physiol,* 218(2): 237–245.

32. Hersel U, Dahmen C, Kessler H, 2003, RGD modified polymers: Biomaterials for stimulated cell adhesion and beyond. *Biomaterials,* 24(24): 4385–4415.

33. Kabsch W, Sander C, 1983, Dictionary of protein secondary structure: Pattern recognition of hydrogen-bonded and geometrical features. *Biopolymers,* 22(12): 2577–2637.

https://doi.org/https://doi.org/10.1002/bip.360221211

34. Lakshmanan A, Hauser CA, 2011, Ultrasmall peptides self-assemble into diverse nanostructures: Morphological evaluation and potential implications. *Int J Mol Sci,* 12(9): 5736–5746.

35. Kikkawa Y, Hozumi K, Katagiri F, *et al.*, 2013, Laminin-111-derived peptides and cancer. *Cell Adhes Migr,* 7(1): 150–159.

36. Kreidberg JA, 2000, Functions of α3β1 integrin. *Curr Opin Cell Biol*, 12(5): 548–553.

37. Khademhosseini A, Camci-Unal G, 2018, *3D Bioprinting in Regenerative Engineering: Principles and Applications*, CRC Press, Boca Raton.

38. Cruz-Acuña R, Quirós M, Farkas AE, *et al.*, 2017, Synthetic hydrogels for human intestinal organoid generation and colonic wound repair. *Nat Cell Biol,* 19(11): 1326–1335.

https://doi.org/10.1038/ncb3632